Global stabilization of high-energy response of a nonlinear wideband electromagnetic energy harvester

T. Sato, S. Kato and A. Masuda

Department of Mechanical and System Engineering, Kyoto Institute of Technology, Matsugasaki, Sakyo-ku, Kyoto, Japan

E-mail: m5623113@edu.kit.ac.jp

Abstract. This paper presents a resonance-type vibration energy harvester with a Duffing-type nonlinear oscillator which is designed to perform effectively in a wide frequency band. For the conventional linear vibration energy harvester, the maximum performance of the power generation and its bandwidth are in a relation of trade-off. Introducing a Duffing-type nonlinearity can expand the resonance frequency band and enable the harvester to generate larger electric power in a wider frequency range. However, since such nonlinear oscillator may have coexisting multiple steady-state solutions in the resonance band, it is difficult for the nonlinear harvester to maintain the high performance of the power generation constantly. The principle of self-excitation and entrainment has been utilized to give global stability to the high-energy orbit by destabilizing other unexpected low-energy orbits by introducing a switching circuit of the load resistance between positive and the negative values depending on the response amplitude of the oscillator. In this paper, an improved control law that switches the load resistance according to a frequency-dependent threshold is proposed to ensure the oscillator to respond in the high-energy orbit without ineffective power consumption. Numerical study shows that the steady-state responses of the harvester with the proposed control low are successfully kept on the high-energy orbit without repeating activation of the excitation-mode.

1. Introduction

A resonance-type vibration energy harvester is an oscillator with electromechanical transducer designed to capture wasted mechanical energy and convert it to electric energy. In the conventional linear design, the natural frequency of the harvester is adjusted to the dominant frequency of the vibration source, and the mechanical Q factor is designed as large as possible in order to maximized the captured power. The Q factor, however, has a trade-off relationship with bandwidth. This trade-off is recognized as one of the most significant issues in resonance-type vibration energy harvester because the actual vibration sources in the environment are likely to have fluctuations in their frequency components. One of the most promising approaches is a Duffing-type nonlinear harvester that uses a nonlinearly sprung mechanical resonator to widen the effective frequency band [1, 2, 3, 4, 5]. This idea is an attempt to develop a single-degree-of-freedom energy harvester which can respond largely in a wide frequency range by folding its resonance peak toward the higher (lower) frequency direction by utilizing a hardening (softening) spring instead of the linear one. This type of nonlinear harvester, however, can have multiple coexisting solutions with different amplitude in the resonance band. If the harvester's response happens to fall into the low-energy orbits, the performance of the harvester can be impaired drastically. Hence, the mechanism that ensures the constant manifestation of the high-energy solution regardless of initial conditions and disturbances is required to maintain the high performance of the nonlinear harvester.

Content from this work may be used under the terms of the Creative Commons Attribution 3.0 licence. Any further distribution of this work must maintain attribution to the author(s) and the title of the work, journal citation and DOI.
Published under licence by IOP Publishing Ltd

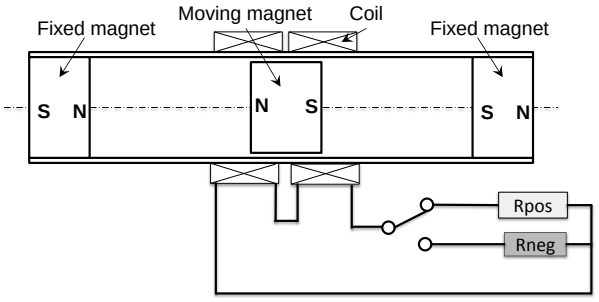


Figure 1. Generalized model of nonlinear vibration energy harvester.

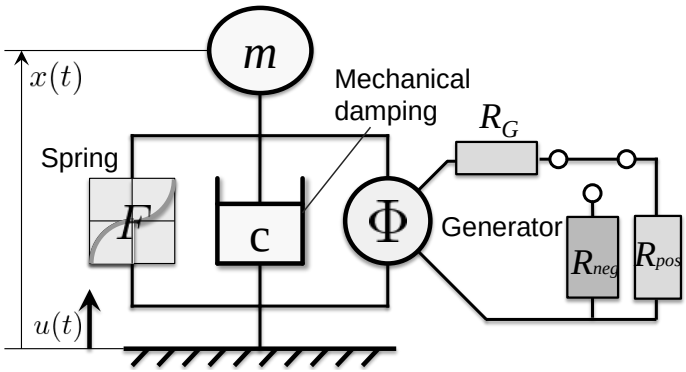


Figure 2. Generalized model of nonlinear vibration energy harvester.

In the previous study [6] presented by the authors, a concept of a nonlinear energy harvester in which only the highest energy solution is globally stabilized has been proposed. This is done by destabilizing other stable solutions by introducing a switching control circuit that switches the load resistance between positive and negative values depending on the response amplitude. This control makes the harvester to behave as a self-induced vibration system, and its ability to synchronize with the external excitation can enable the harvester to respond stably in the highest-energy orbit. In addition, the threshold value for the switching control determines in what level the self-induced limit cycle oscillation occurs, so that the threshold value lager than the amplitudes of the unfavorable low-energy orbits can destabilize them. As a consequence, only the highest-energy trajectory can be stable.

Although it was suggested in the previous study [6] that the adequate value of the threshold might depend on the input frequency, the threshold level was set constant. In this study, the dependence of the appropriate threshold value on the input frequency is mainly investigated. The domain of attraction of the high-energy solution is first studied at various combination of frequencies and thresholds, and an approximate function which describes the desirable threshold value in function of the input frequency is empirically obtained.

2. Magnetically sprung nonlinear energy harvester

Figure 1 illustrates the electromagnetic vibration energy harvester investigated in this study. It consists of plastic cylinder which has a pair of permanent magnets mounted at both ends and a moving permanent magnet enclosed inside. The polarities of the magnets are set so that the moving magnet receives repulsive forces from fixed magnets. Copper wire is wound outside the cylinder to make a solenoid coil that performs as a stator of the generator. The three magnets comprise a magnetic hardening spring, and the center moving magnet not only acts as an inertial mass but also provides moving magnetic flux

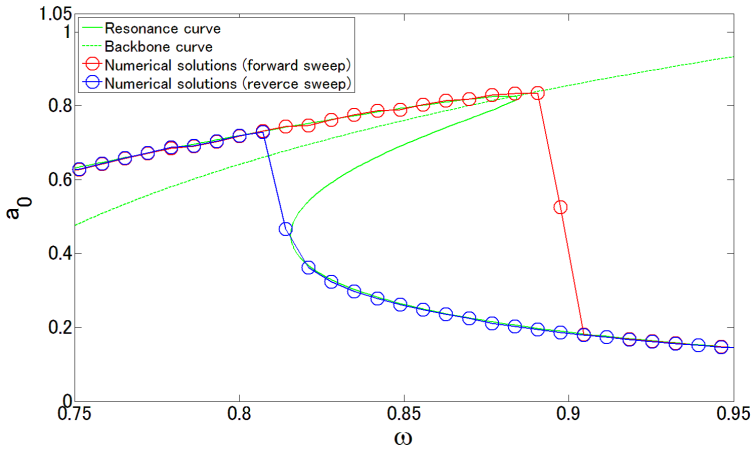
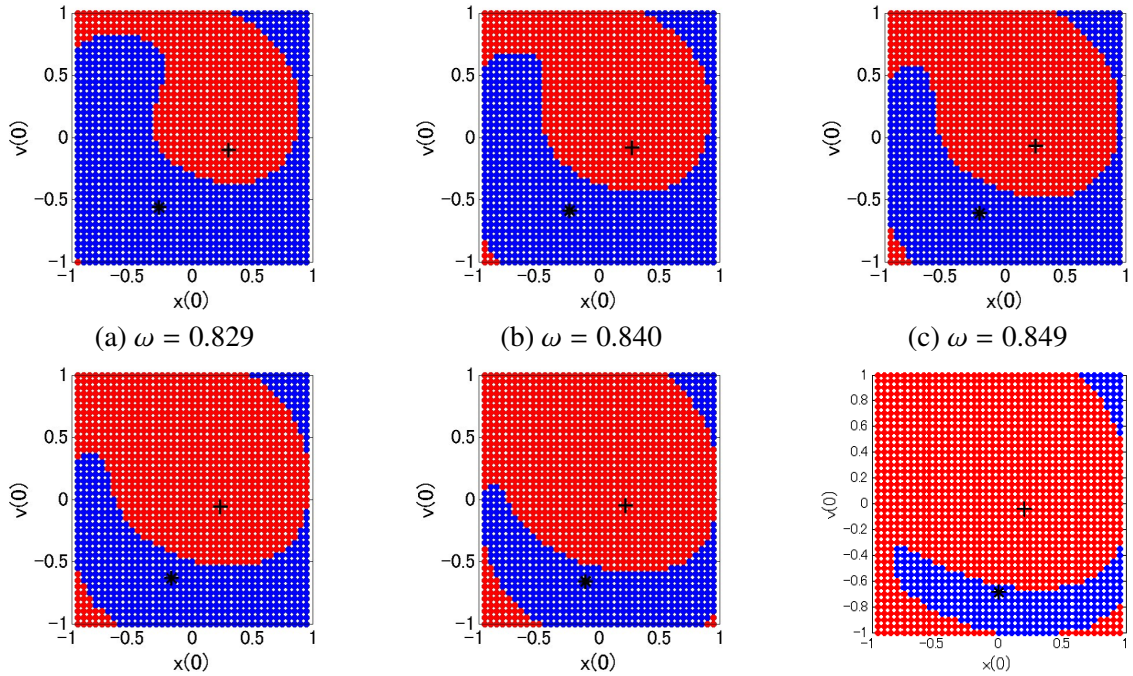


Figure 3. Resonance curve without load resistance switching control for $u_a = 0.0628$ and $\rho = 1.90$



(a) $\omega = 0.829$ (b) $\omega = 0.840$ (c) $\omega = 0.849$

(d) $\omega = 0.858$ (e) $\omega = 0.870$ (f) $\omega = 0.884$

Figure 4. Basins of attraction of high-energy solution low-energy solution without load resistance switching control for $u_a = 0.0628$ and $\rho = 1.90$

through the coil.

This harvester is modeled as a single-degree-of-freedom nonlinear mechanical oscillator with an electromagnetic transducer followed by a load circuit as schematically illustrated in Figure 2. The equation of motion combined with the circuit equation in a dimensionless form is derived as [6]

$$\ddot{x}(t) + 2\left(\zeta_m + \zeta_e \frac{\left\{1 + \Phi_{NL}(x(t))^2\right\}}{1 + \rho(x(t), \dot{x}(t))}\right)\dot{x}(t) + x(t) + F_{NL}(x(t)) = -u_a \cos \omega t \tag{1}$$

where ζ_m, ζ_e, ρ, x, u_a, and ω denote the mechanical damping ratio, the electrical damping ratio, the dimensionless load resistance, the dimensionless displacement of the moving magnet, the dimensionless

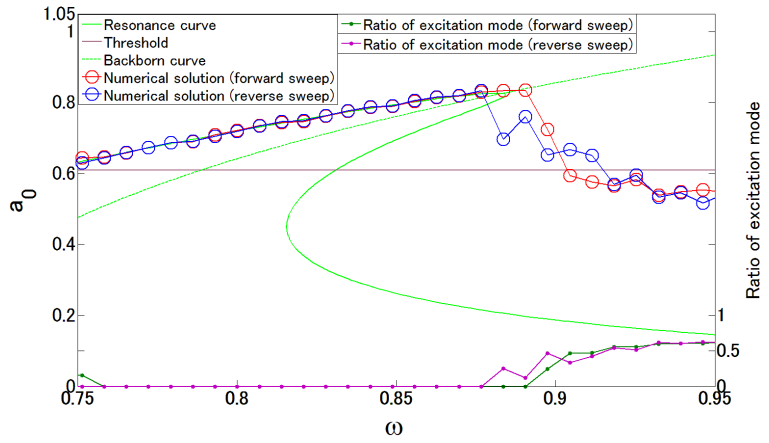


Figure 5. Resonance curve with load resistance switching control for $u_a = 0.0628$, $\rho_{pos} = 1.90$, $\rho_{neg} = -1.90$, and $a_{th} = 0.6$

amplitude of the input acceleration, and the dimensionless input frequency, respectively. The nonlinear functions Φ_{NL} and F_{NL} represent the dimensionless nonlinear force factor and the dimensionless nonlinear restoring force, respectively.

3. Global stabilization of high-energy response by frequency-dependent load resistance switching

3.1. Coexistence of stable steady-state responses

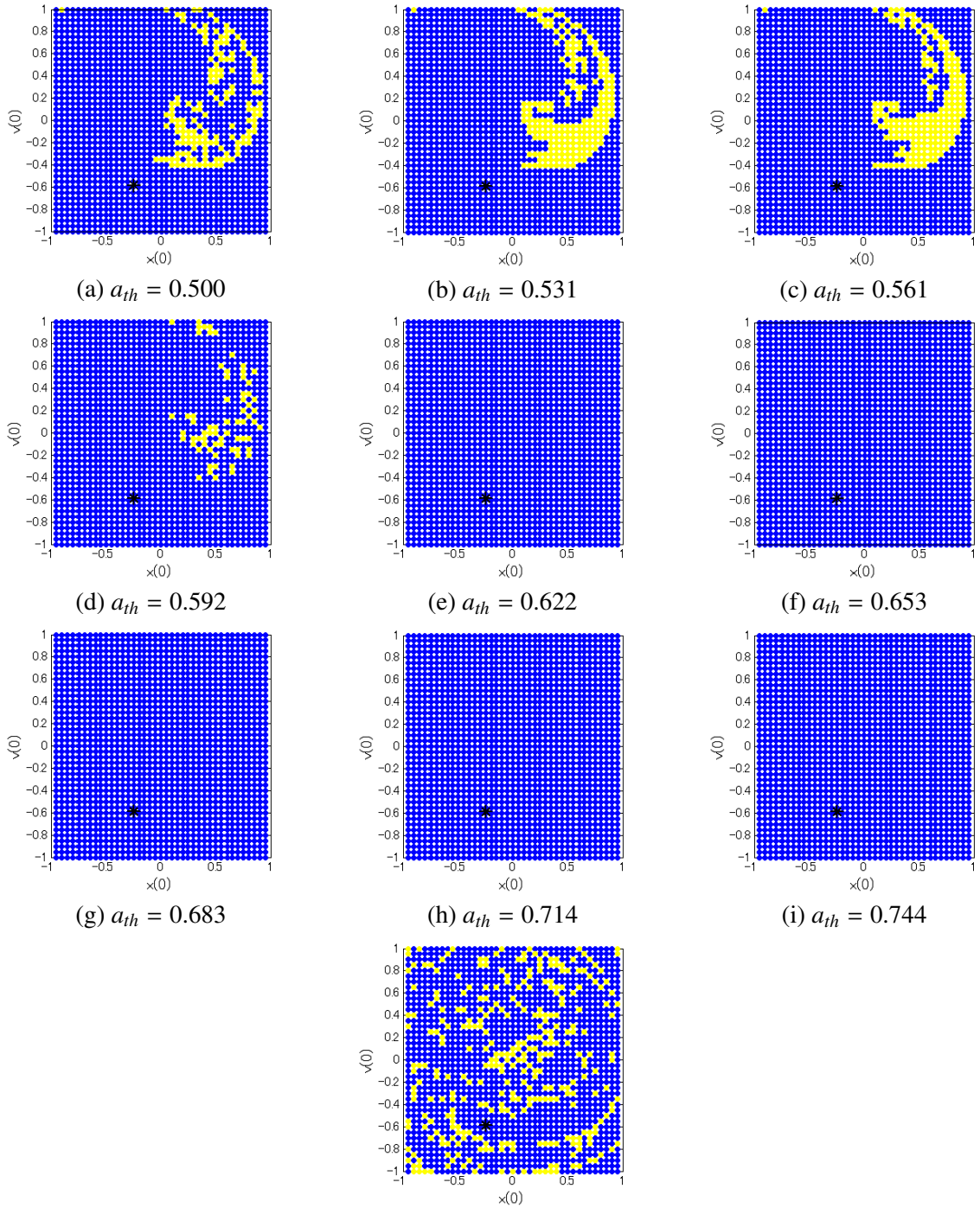
A vibratory system with a nonlinear stiffness may have multiple stable solutions with different amplitude in the resonance band when it is subjected to a sinusoidal excitation. It depends on the initial conditions to which solution the response converges in the steady-state. Figure 3 shows a numerically calculated steady-state solutions with a theoretically derived resonance curve using the averaging method for the input acceleration of $u_a = 0.0628$ and the load resistance of $\rho = 1.90$. In the plot, one can see that two stable solutions (high- and low-energy solutions) and one unstable solution between them coexist in the band from $\omega = 0.815$ to $\omega = 0.884$. Figure 4 shows the basins of attraction of these two stable solutions on the Poincaré section at $2\pi n$ ($n \in Z$) for the excitation frequencies of 0.829, 0.840, 0.849, 0.858, 0.870, and 0.884. The blue and red circles indicate that these lattice points belong to the basins of the high- and low-energy solutions, respectively. The steady-state solutions on the Poincaré section are indicated by "+" (low-energy solution) and "*" (high-energy solution).

3.2. Stabilization of high-energy response by load resistance switching

As shown in Figures 3 and 4, two stable steady-state solutions coexist near the resonance peak, and the initial conditions determine which solution emerges. Therefore, the nonlinear energy harvester can generate high power as long as it remains in the high-energy orbit, but once it falls down to the low-energy orbit due to the disturbance, its performance fatally detracts. Thus, some mechanism is required that forces the harvester always respond in the hight-energy orbit to assure the advantageous performance.

In the previous study [6], the principle of forced entrainment of the self-induced oscillator was introduced to destabilize the low-energy solution and to lead any response to the hight-energy solution, regardless of the initial conditions and the disturbances. Specifically, a load resistance switching control is introduced which varies the load resistance positive to negative by switching the circuit when the response amplitude is smaller than a threshold, and vice versa:

$$\rho = \begin{cases} \rho_{pos} & (a \geq a_{th}); \quad \text{harvesting-mode} \\ \rho_{neg} & (a < a_{th}); \quad \text{excitation-mode} \end{cases} \tag{2}$$



(a) $a_{th} = 0.500$ (b) $a_{th} = 0.531$ (c) $a_{th} = 0.561$

(d) $a_{th} = 0.592$ (e) $a_{th} = 0.622$ (f) $a_{th} = 0.653$

(g) $a_{th} = 0.683$ (h) $a_{th} = 0.714$ (i) $a_{th} = 0.744$

(j) $a_{th} = 0.775$

Figure 6. Basins of attraction of high-energy and quasiperiodic solutions with load resistance switching control for $u_a = 0.0628$, $\rho_{pos} = 1.90$, $\rho_{neg} = -1.90$, and $\omega = 0.840$

where a is the displacement amplitude of the oscillator, and a_{th} is a threshold value. ρ_{pos} is the load resistance, while ρ_{neg} is a negative resistance which performs as a energy source to excite the oscillator. The negative resistance is to be implemented as a negative impedance converter (NIC) circuit.

Table 1. Values of excitation frequency and threshold

ω	a_{th}									
0.829	0.500	0.527	0.553	0.580	0.606	0.633	0.659	0.686	0.712	0.739
0.840	0.500	0.528	0.556	0.584	0.612	0.640	0.668	0.696	0.724	0.752
0.849	0.500	0.529	0.559	0.588	0.617	0.647	0.676	0.705	0.734	0.764
0.858	0.500	0.531	0.561	0.592	0.622	0.653	0.683	0.714	0.744	0.775
0.870	0.500	0.532	0.564	0.596	0.627	0.659	0.691	0.723	0.755	0.787
0.884	0.500	0.533	0.565	0.598	0.631	0.663	0.696	0.728	0.761	0.794

Figure 5 shows the resonance curve with the load resistance switching control with a fixed threshold of 0.6. Since this control law imparts the self-excitation capability to the oscillator to perform an entrainment into the highest-energy solution, the low-energy branch successfully turns unstable and never appear in the numerical responses. Around the tip of the resonance peak (from $\omega = 0.870$ to 0.884), however, there remains some hysteresis and the responses seem unsteady. This implies that the system shows quasiperiodic response in this region, in which the entrainment breaks and the limit cycle and the forced response emerge simultaneously. Because the circuit in these cases is repeatedly switched to the excitation-mode as shown in the plot (right axis), the system ineffectively consumes the harvested power to drive the NIC.

Figure 6 shows the basins of attraction of high-energy and quasiperiodic solutions on the Poincaré section at $2\pi n$ ($n \in Z$) with the load resistance switching control with various threshold values for the excitation frequency of 0.840. Blue and yellow circles indicate that these points belong to the basins of the high-energy and quasiperiodic solutions, respectively. When the threshold value is too small, there exists the basin of the quasiperiodic solution with a complex fractal-like shape. For the threshold larger than 0.622, the basin of the quasiperiodic solution disappears, and the high-energy solution earns global stability, except for the threshold value of 0.775 where the quasiperiodic solution again emerges.

3.3. Frequency-dependent switching

The above results suggest that there may be an appropriate range of the threshold value for the sake of global stability, and it may depends on other parameters especially on the excitation frequency. Hence, more comprehensive examination is conducted in terms of the appropriate threshold value in function of the excitation frequency. The values of the threshold and the input frequency investigated are listed in

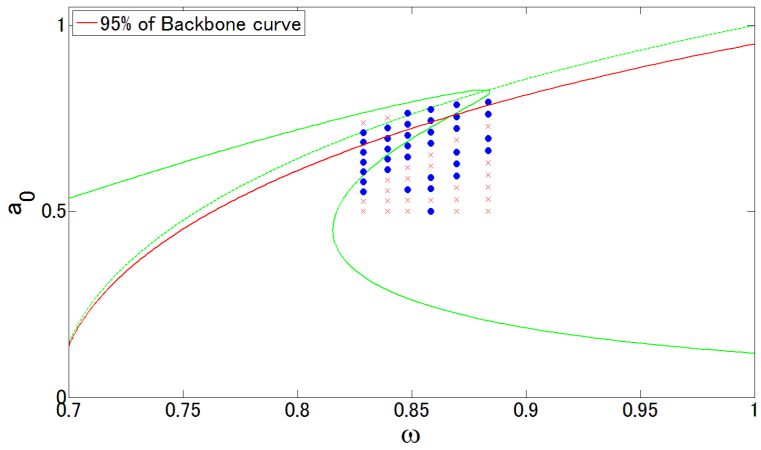


Figure 7. Relation of thresholdvalue and global stability of large-amplitude solution for $u_a = 0.0628$, $\rho_{pos} = 1.90$, $\rho_{neg} = -1.90$

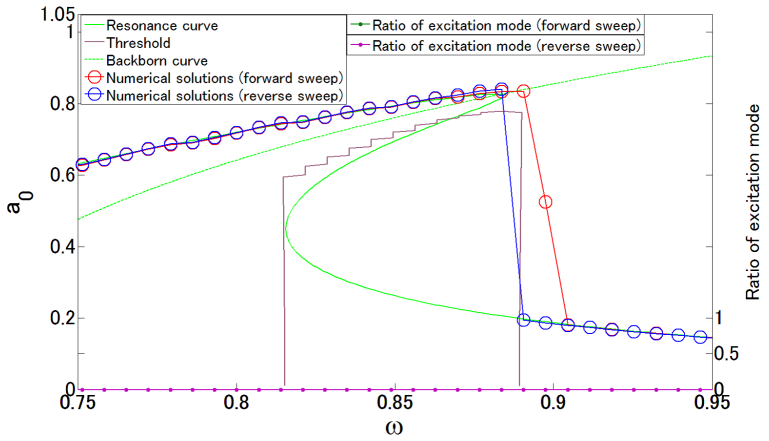


Figure 8. Resonance curve with frequency-dependent load resistance switching control for $u_a = 0.0628$, $\rho_{pos} = 1.90$, $\rho_{neg} = -1.90$

Table 1.

Figure 7 shows the results. In the figure, the blue dots indicate that the high-energy solution shows the global stability for the same range of initial conditions as shown in Figure 6, while the red crosses indicate the existence of the basin of the quasiperiodic solutions. It seems that the curve of 95 % of the backbone curve indicated by a red line in the figure is a reasonable approximation of the appropriate threshold level in this case. The third-order approximation of this curve is derived as follows:

$$a_{th}(\omega) = 18.27(\omega)^3 - 52.69(\omega)^2 + 51.95\omega - 16.59 \tag{3}$$

In addition, since the load resistance switching control is unnecessary in the frequency range where there exists merely one stable solution, the threshold value should be set to zero. Therefore,

$$a_{th}(\omega) = \begin{cases} 18.27(\omega)^3 - 52.69(\omega)^2 + 51.95\omega - 16.59 & (0.815 \leq \omega \leq 0.884) \\ 0 & (otherwise) \end{cases} \tag{4}$$

Figure 8 shows the numerically calculated steady-state responses of the harvester with the proposed frequency-dependent switching control. The response is successfully kept on the high-energy orbit without continuous power consuming due to the repeating activation of the excitation-mode.

4. Conclusions

In this paper, the concept of the wide-band nonlinear energy harvester with the load resistance switching control has been presented in order to overcome the limitation of this type of nonlinear energy harvesters caused by the existence of multiple stable solutions in the resonance band. A control law that switches the load resistance between positive and negative values according to the comparison of the oscillator's amplitude with the frequency-dependent threshold has been proposed to ensure the oscillator to respond in the high-energy orbit. It has been presented that the numerically calculated steady-state responses of the harvester with the proposed control low are successfully kept on the high-energy orbit without ineffective power consumption due to the repeating activation of the excitation-mode.

5. Reference

[1] Tang L, Yang Y and Soh C K 2010 Toward broadband vibration-based energy harvesting, *Journal of Intelligent Material Systems and Structures* 21(18), pp 1867–1897.

[2] Soliman M S M , Abdel-Rahman E M , El-Saadany E F and Mansour R R 2008 A Wideband Vibration-Based Energy Harvester, *Journal of Micromechanics and Microengineering* 18(11), p 115021.

[3] Ferrari M, Ferrari V, Guizzetti M, And'o B, Baglio S, and Trigona C 2009 Improved energy harvesting from wideband vibrations by nonlinear piezoelectric converters, *Procedia Chemistry* 1(1), pp 1203 – 1206.
[4] Stanton S C, McGehee C C, and Mann B P 2009 Reversible hysteresis for broadband magnetopiezoelastic energy harvesting, *Applied Physics Letters* 95(17), p 174103.
[5] Karami M A and Inman D J 2010 Nonlinear hybrid energy harvesting utilizing a piezo-magneto-elastic spring, *in Proceedings of SPIE*, 7643, p 76430U.
[6] Masuda A, Senda A, Sanada T, and Sone A 2013 Global stabilization of high-energy responce for a Duffing-type wideband nonlinear energy harvester via self-excitation and entrainment, *Journal of Intelligent Material Systems and Structures*, Vol.24, No.13, pp 1589–1612.